Accepted Manuscript

Zirconium catalyzed synthesis of 2-arylidene Indan-1,3-diones and evaluation of their inhibitory activity against NS2B-NS3 WNV protease

Ana Flávia C. da S. Oliveira, Ana Paula M. de Souza, André S. de Oliveira, Milene L. da Silva, Fabrício M. de Oliveira, Edjon G. Santos, Ítalo Esposti P. da Silva, Rafaela S. Ferreira, Filipe S. Villela, Felipe T. Martins, Daniel H.S. Leal, Boniek G. Vaz, Róbson R. Teixeira, Sergio O. de Paula

PII: S0223-5234(18)30167-3

DOI: 10.1016/j.ejmech.2018.02.037

Reference: EJMECH 10214

To appear in: *European Journal of Medicinal Chemistry*

Received Date: 22 November 2017

Revised Date: 2 February 2018

Accepted Date: 10 February 2018

Please cite this article as: Ana.Flá.C.da.S. Oliveira, A.P.M. de Souza, André.S. de Oliveira, M.L. da Silva, Fabrí.M. de Oliveira, E.G. Santos, Í.Esposti.P. da Silva, R.S. Ferreira, F.S. Villela, F.T. Martins, D.H.S. Leal, B.G. Vaz, Ró.R. Teixeira, S.O. de Paula, Zirconium catalyzed synthesis of 2-arylidene Indan-1,3-diones and evaluation of their inhibitory activity against NS2B-NS3 WNV protease, *European Journal of Medicinal Chemistry* (2018), doi: 10.1016/j.ejmech.2018.02.037.

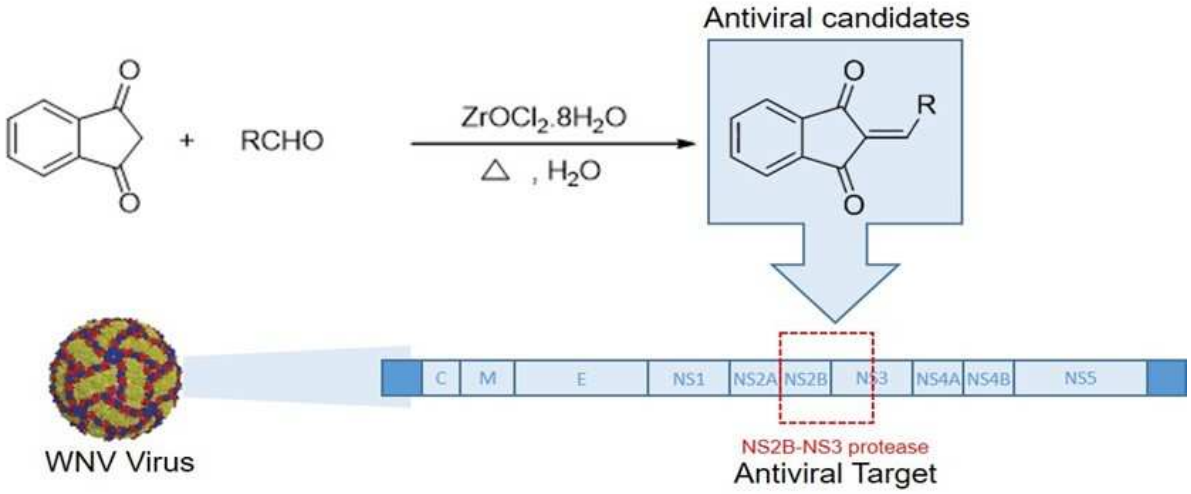

ZIRCONIUM CATALYZED SYNTHESIS OF 2-ARYLIDENE INDAN-1,3-DIONES AND EVALUATION OF THEIR INHIBITORY ACTIVITY AGAINST NS2B-NS3 WNV PROTEASE

Ana Flávia C. da S. Oliveira, ‡ [a,b] Ana Paula M. de Souza, ‡ [c] André S. de Oliveira, ‡ [a,b] Milene L. da Silva,[c] Fabrício M. de Oliveira,[d] Edjon G. Santos,[a] Ítalo Esposti P. da Silva,[a] Rafaela S. Ferreira,[e] Filipe S. Villela,[e] Felipe T. Martins,[f] Daniel H. S. Leal,[g] Boniek G. Vaz,[f] Róbson R. Teixeira,*[c] and Sergio O. de Paula*[a]

[a] Departamento de Biologia Geral, Universidade Federal de Viçosa, Av. P.H. Rolfs, S/N, 36570-900 – Viçosa (Brazil).

[b] Instituto Federal de Educação, Ciência e Tecnologia do Norte de Minas, 39101-000 – Diamantina (Brazil).

[c] Departamento de Química, Universidade Federal de Viçosa, Av. P.H. Rolfs, S/N, 36570-900 – Viçosa (Brazil).

[d] Instituto Federal de Minas Gerais (IFMG), Campus Ouro Branco Rua Afonso Sardinha, 90, 36420-000, Ouro Branco (Brazil).

[e] Departamento de Bioquímica e Imunologia, Universidade Federal de Minas Gerais, Av. Antônio Carlos 6627, 31270901 – Belo Horizonte (Brazil).

[f] Instituto de Química, Universidade Federal de Goiás, Av. Esperança, s/n, Campus Samambaia, 74690-970, Goiânia (Brazil).

[g] Centro Universitário Norte do Espírito Santo, Universidade Federal do Espírito Santo, Rodovia BR 101 Norte, Km 60 - Bairro Litorâneo, 29932-900 - São Mateus (Brazil).

‡These authors contributed equally.

***Corresponding Authors**

Sérgio Oliveira de Paula (depaula@ufv.br): Departamento de Biologia Geral, Universidade Federal de Viçosa, Av. P.H. Rolfs, S/N, 36570-900 – Viçosa (Brazil), Tel./Fax: +55-31-3899-2589; and Róbson Ricardo Teixeira (robsonr.teixeira@ufv.br): Universidade Federal de Viçosa, Av. P.H. Rolfs, S/N, 36570-900 – Viçosa (Brazil), Tel./Fax: +55-31-3899-3209.

KEYWORDS: antiviral agents; West Nile Virus; indan-1,3-dione; Knoevenagel condensation.

ABSTRACT: A simple and efficient Knoevenagel procedure for the synthesis of 2-arylidene indan-1,3-diones is herein reported. These compounds were prepared via ZrOCl2·8H2O catalyzed reactions of indan-1,3-dione with several aromatic aldehydes and using water as the solvent. The 2-arylidene indan-1,3-diones were obtained with 53%-95% yield within 10-45 minutes. The synthesized compounds were evaluated as inhibitors of the NS2B-NS3 protease of West Nile Virus (WNV). It was found that hydroxylated derivatives impaired enzyme activity with varying degrees of effectiveness. The most active hydroxylated derivatives, namely 2-(4-hydroxybenzylidene)-1*H*-indene-1,3(2*H*)-dione (**14**) and 2-(3,4-dihydroxybenzylidene)-1*H*-indene-1,3(2*H*)-dione (**17**), were characterized as noncompetitive enzymes inhibitors, with IC_{50} values of 11 μmol L^{-1} and 3 μmol L^{-1}, respectively. Docking and electrostatic potential surfaces investigations provided insight on the possible binding mode of the most active compounds within an allosteric site.

INTRODUCTION

The formation of carbon-carbon bonds (single, double and triple) is one of the most important aspects in organic chemistry. Several methodologies have been developed to achieve the formation of these bonds, and the Knoevenagel condensation is a synthetically useful carbon-carbon forming transformation [1-3]. This reaction involves condensation between activated methylene- and carbonyl-containing compounds. The Knoevenagel reaction has been explored in organic synthesis for the preparation of several classes of compounds, such as coumarines which are important intermediates in the synthesis of pharmaceuticals, cosmetics, and perfumes [4, 5]. In addition, this reaction has been used in the total synthesis of natural compounds such as the illudalane sesquiterpene illudinine [6]. Typically, the Knoevenagel condensation is carried out in the presence of weak bases such as ethylenediamine, piperidine or ammonium salts. Over the years, several modifications of this reaction have been reported, including the use of Lewis acids [7].

Zirconyl chloride is a Lewis acid that has drawn much attention of organic chemists because of its water stability, low toxicity, and commercial availability. As a consequence, this oxysalt has been applied in several organic transformations such as oxidation of alcohols [8], esterification of carboxylic acids [9], synthesis of 2-aryloxazolines and *bis*-oxazolines [10], preparation of enaminones and enamino esters [11], among others [11-22]. As can be noticed, Zirconyl chloride

is a useful catalyst that can be utilized in a variety of transformations, such as the Knoevenagel methodology presented in this investigation which resulted in the discovery of indan-1,3-dione derivatives endowed with Flavivirus protease inhibitory activity.

The Flavivirus genus encompasses a group of enveloped RNA arthropod-borne viruses (arboviruses) responsible for important human and animal diseases caused by virus like Yellow Fever Virus (YFV), Zika Virus (ZIKV), Dengue Virus (DENV), West Nile Virus (WNV), Japanese Encephalitis Virus (JEV), Tick-Borne Encephalitis Virus (TBEV), and Kyasanur Forest Disease Virus (KFDV) [23].

WNV infection represents a serious burden to human and animal health because of the virus capability to cause unforeseen and large epidemics. Cases of WNV infection were limited to European, Asian and African countries until 1999, when the virus reached the Western Hemisphere [24, 25]. Within three years, the virus spread to Canada and Mexico, followed by animal and human cases in Central and South America [26-28].

WNV is an enveloped virus whose genome consists of a single-stranded RNA with positive polarity and approximately 11 kb. It contains a single open reading frame encoding a precursor polyprotein, which is processed by viral and host proteases, giving rise to three structural proteins, namely capsidial protein (C), envelope glycoprotein (E) and pre-membrane/membrane protein (prM/M). The RNA also encodes seven non-structural proteins, NS1, NS2A, NS2B, NS3, NS4A, NS4B and NS5, which are involved in the replicative cycle of the virus[29].

Viral protease is responsible for the cleavage of some sites, including NS2A-NS2B, NS2B-NS3, NS3-NS4A, NS4B-NS5. It also cleaves the signal sequences at the C-prM position and the NS4A-NS4B, within NS2A, and within the NS3 itself [30, 31].

Viral enzymes are important targets for therapeutic intervention and they have been explored towards the development of antiflavivirals [31-33]. As a consequence, research groups have identified reversible and irreversible inhibitors for Flavivirus proteases [34-38].

Within this context, we report herein a simple and efficient zirconium catalyzed Knovenagel procedure for the synthesis of 2-arylidene-indan-1,3-diones. The synthesized compounds were evaluated as inhibitors of the NS2B-NS3 protease of West Nile Virus (WNV) and the results are discussed. This investigation was conducted in order to assess the possibility of using these derivatives as antiviral for the treatment of diseases caused by Flaviridae viruses. It was found that the hydroxylated derivatives impaired enzyme activity with varying degrees of effectiveness.

Docking and electrostatic potential surfaces investigations provided insights about the way the most active compounds act by inhibiting the activity of this enzyme.

RESULTS AND DISCUSSION

Synthesis of 2-arylidene-indan-1,3-diones: The reaction of indan-1,3-dione and 4-chlorobenzaldehyde was chosen as the model reaction for optimization of the catalytic system and reaction conditions. All the reactions were performed in air and the results are shown in Table 1.

Table 1. Knoevenagel condensation reactions of 4-chlorobenzaldehyde and indan-1,3-dione under different conditions

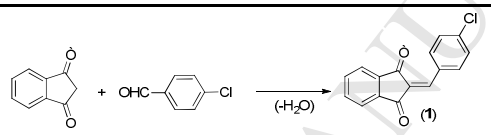

Entry	Heating source	Reagent ratio (in mmol)	Catalyst loading (mol%)	Solvent	Temperature (°C)	Reaction time (min)	Yield (%)
1	Oil bath	1:1	4	free	85	70	33
2	Oil bath	1:1.2	4	free	85	90	31
3	MW	1:1	4	free	85	30	36
4	Oil bath	1:1	4	water	85	65	68
5	MW	1:1	4	water	85	30	70
6	Oil bath	1:1	4	water	40	120	86
7	Oil bath	1:1	4	water	r.t.	480	83
8	Oil bath	1:1	2	water	85	110	84
9	Oil bath	1:1	8	water	85	30	66
10	Oil bath	1:1	-	water	85	420	27

MW = microwave irradiation; r.t. = room temperature

We started the optimization process running a solvent free reaction at 85 ^{o}C, using 1 mmol of each reagent, 4 mol% of $ZrOCl_2 \cdot 8H_2O$, and oil bath conventional heating. After 70 min, the 4-chlorobenzylidene indan-1,3-dione (**1**) was obtained with 33% yield after recrystallization (Entry 1). Increasing the amount of 4-chlorobenzaldehyde (1.2 mmol, Entry 2) did not improve the yield. Compound **1** was obtained with 36% yield when the reaction was conducted under microwave irradiation and in the absence of solvent (Entry 3). When water was used as solvent, the yield of the reaction was substantially increased (Entries 4 and 5) compared to the reactions performed in the absence of solvents. For the sack of simplicity, we decided to continue the optimization process employing conventional heating, despite the shorter reaction time under microwave irradiation. Decreasing reaction temperature (Entries 6 and 7) resulted in longer reaction times albeit with better yields compared to the reaction condition of Entry 4. By reducing the catalyst loading to 2 mol%, compound **1** was obtained in 84% yield after 110 minutes (Entry 8). Doubling the amount of catalyst to 8 mol% (Entry 9), the reaction time was reduced and the yield was about the same compared to reaction of Entry 4; however, the reaction work up was troublesome. To verify the impact of the zirconium catalyst, we also run the reaction in its absence (Entry 10). As expected, the reaction time was substantially increased and the product was obtained only with 27% yield, reinforcing the importance of the catalytic effect of $ZrOCl_2 \cdot 8H_2O$.

Since reaction conditions of entry 4 afforded compound **1** with synthetically useful yield, simple workup and shorter period of time (compared to other reactions herein conducted with conventional heating), they were after applied in order to investigate the scope of the zirconium catalyzed Knoevenagel reaction to prepare 2-arylidene indan-1,3-diones. Fifteen compounds were synthesized (Scheme 1) and obtained in synthetically useful yields (53%–95%) within 10–45 minutes (see Table 1S in the Supporting Information). These indan-1,3-dione derivatives comprised compounds containing electron-donating and electron withdrawing groups attached to the aromatic ring of arylidene portion. A heterocyclic derivative (compound **9**) was also prepared. It should be mentioned that interesting heterocycle scaffolds can be accessed from compounds containing active methylene moieties via condensation of them with aromatic aldehydes as described, for instance, by Elmuradov and co-workers[39].

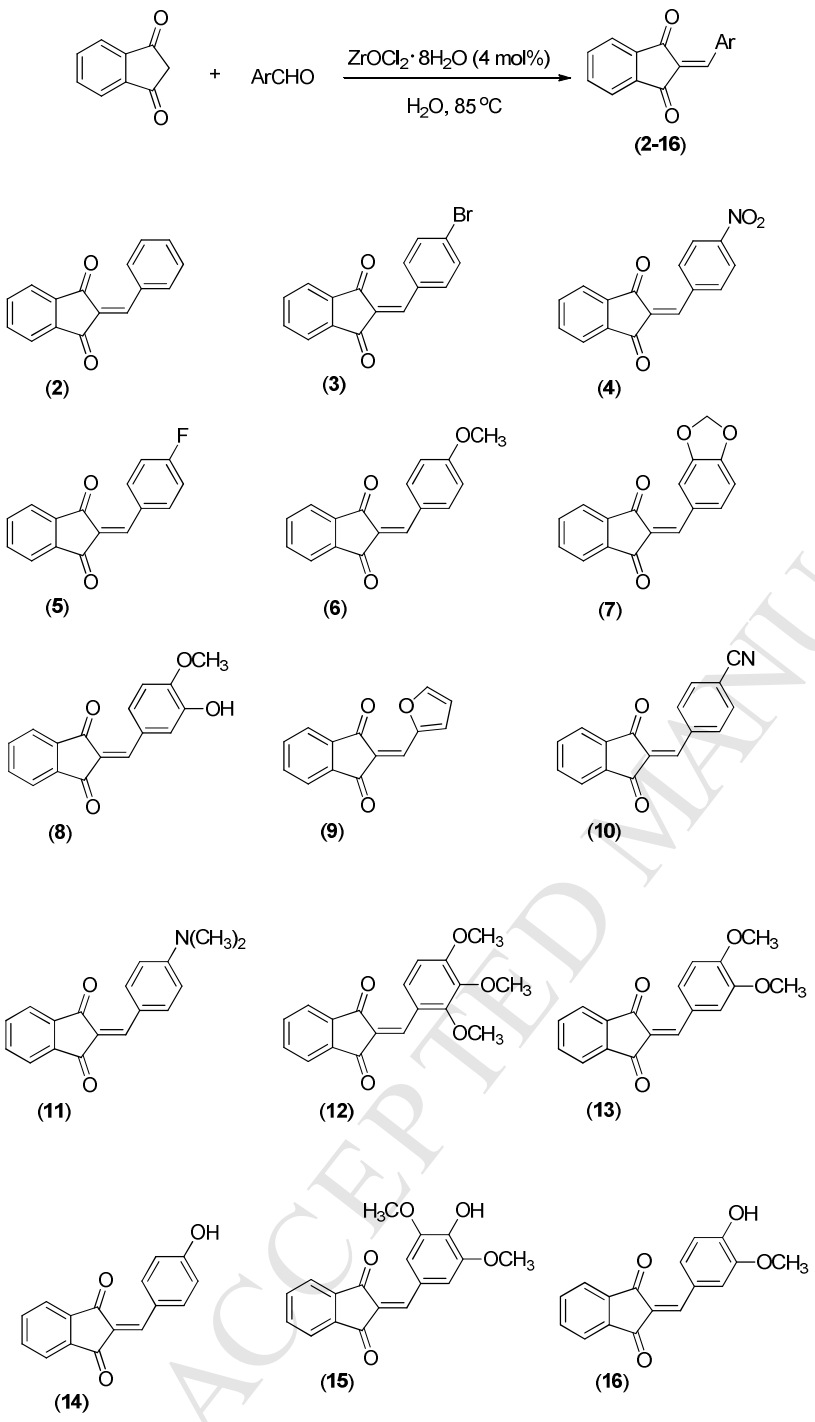

Scheme 1. Structures of indan-1,3-diones **2**–**16**.

The derivative 2-(3,4-dihydroxybenzylidene)-1*H*-indene-1,3(2*H*)-dione (**17**) was prepared, in 58% yield, via dimethylation of compound **13** using BBr_3 (Scheme 2).

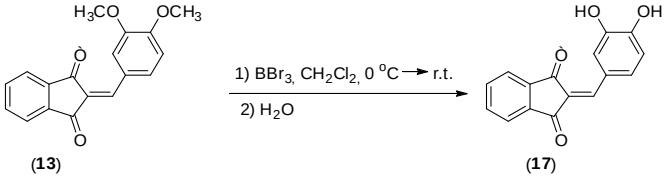

Scheme 2. Preparation of compound **17**.

The identities of substances **1**–**17** were confirmed by IR and NMR spectroscopy as well as mass spectrometry. In the IR spectrum, two bands, one observed within 1709–1731 cm^{-1} and the other within 1655–1688 cm^{-1} range, were attributed to the carbonyl groups. Two signals at approximately 190 ppm in the ^{13}C NMR spectra confirmed the presence of the carbonyl groups in the structures of compounds **1**–**17**. The substitution patterns of the aromatic rings in the arylidene portions were compatible with the ^{1}H NMR spectra.

We were able to obtain a monocrystal of compound **15**. Considering that X-ray information can be useful in terms of structure activity-relationship, we have also determined its crystal structure. A summary of crystal data collect and processing is presented in the Supporting Information (Table 2s). Compound **15** has crystallized in the centrosymmetric monoclinic space group $P2_1/c$ with just one molecule in the asymmetric unit (Figure 1), which is almost planar (root mean square deviation of all non-hydrogen atoms is 0.0532 Å, with the largest atom deviation from the least-square plane of 0.202(5) Å for C18).

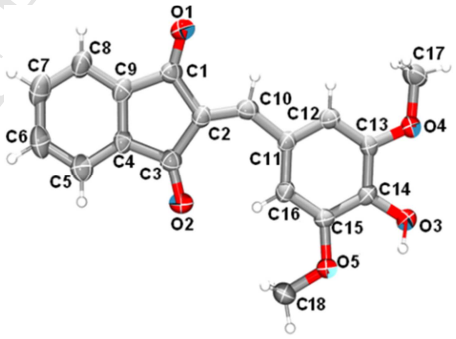

Figure 1. 30% ellipsoid plot for non-hydrogen atoms of compound **15** in its crystal structure. Hydrogens were drawn as arbitrary radius spheres. Atom labeling scheme is arbitrary.

The crystal packing of **15** is mainly stabilized through the formation of one-dimensional chains assembled with 2_1-axis symmetry related molecules along the crystallographic axis *b*. In these chains, there is one classical intermolecular hydrogen bond between the hydroxyl group (donor) and one carbonyl oxygen (acceptor), besides one non-classical hydrogen bond involving a CH aromatic moiety (donor) and one methoxy oxygen (acceptor) (Figure 2).

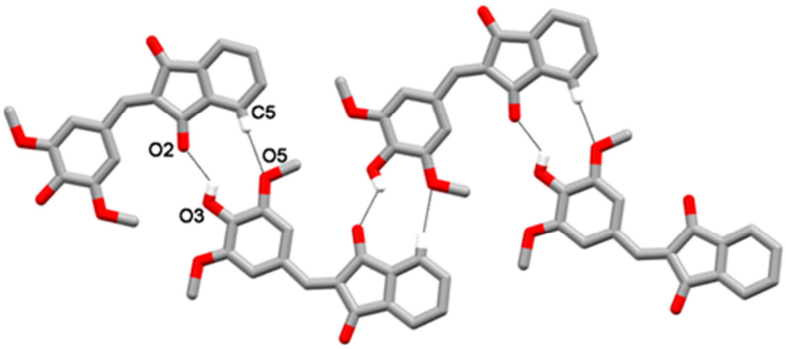

Figure 2. One-dimensional chain found in the crystal packing of compound **15**. Just the hydrogen bonding (black lines) donor and acceptor atoms were labeled only once.

Biological activity assays and Computational analyses: The evaluation of the inhibitory effect of compounds **1**–**17** on NS2B-NS3 WNV enzyme was carried out *via* a fluorogenic substrate assay. Initially, the enzyme was incubated for 30 minutes with the compounds under evaluation. Subsequently, reactions were initiated with the addition of the substrate pERTKRAMC. Among the evaluated indan-1,3-dione derivatives, compounds **14** and **17** showed inhibitory behavior, with reduction of 41% and 100% of the enzymatic activity, respectively, at the concentration of 16 μmol L^{-1} (Figure 3). These compounds present, as a common structural feature, a hydroxyl group at the *para* position of the aromatic ring of the arylidene moiety. Moreover, compound **17**, which displayed the best inhibitory response, possesses an additional hydroxyl group at the *meta* position. Previous investigations conducted with HIV protease have demonstrated that hydroxyl groups would be important for inhibiting the replication of this virus. Effective HIV protease inhibitors had a hydroxyl group that replaced the water molecule from the catalytic active-center. In this case, the hydroxyl group established hydrogen bonding with catalytically active aspartates[40]. Tomlinson and Watowich demonstrated the involvement of the hydroxyl group in DENV protease inhibition. Significant interactions occurred between

hydroxyl groups of inhibitors with preserved residues that constitute the catalytic triad (His^{51}, Asp^{75}, Ser^{135}) of the protease[41].

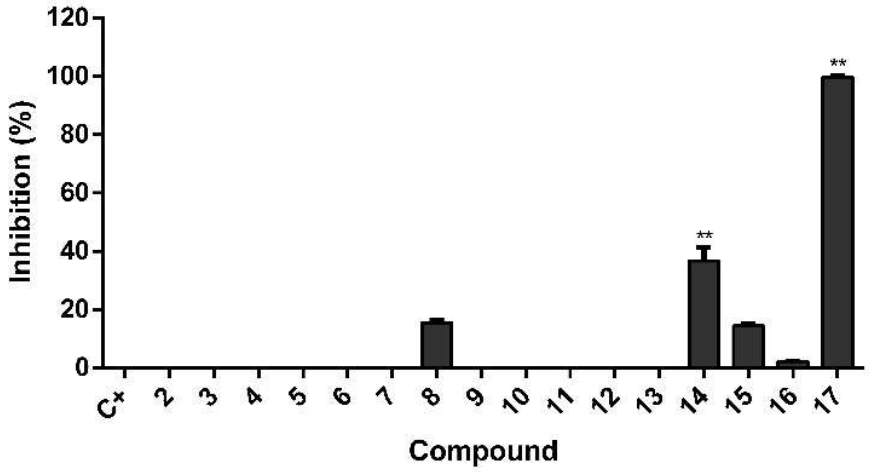

Figure 3. Antiviral screening for WNV protease: seventeen indan-1,3-dione derivatives were evaluated in at the concentration of 16 μmol L^{-1} against WNV NS2-NB3 protease. p value < 0.0001. ** indicates statistical significance. The assays were conducted in triplicated on three isolated experiments.

In order to obtain the inhibitory concentration of the compounds that reduces activity by 50% (IC_{50}), enzymatic inhibition of the NS2-NB3 WNV protease was evaluated under varying concentrations of the most active compounds **14** and **17**. Both these indan-1,3-dione derivatives showed dose-response inhibition with IC_{50} values of 11 μmol L^{-1} and 3 μmol L^{-1}, respectively.

With the aim of verifying the possible mechanism of inhibition by these compounds, enzyme kinetic assays were conducted under varying substrate concentrations and three concentrations of each compound (2, 4 and 8 μmol L^{-1}). Compounds **14** and **17** promoted a significant decrease in the maximum enzymatic velocity without changes in K_M values as depicted in Figure 4. The Lineweaver-Burk plot presented lines intersecting on the x-axis for both compounds. K_i values were 12.31 μmol L^{-1} and 1.25 μmol L^{-1} for **14** and **17**, respectively. This inhibition profile suggests a noncompetitive inhibition mode of action, in which the inhibitor and the substrate can bind simultaneously to an enzyme molecule.

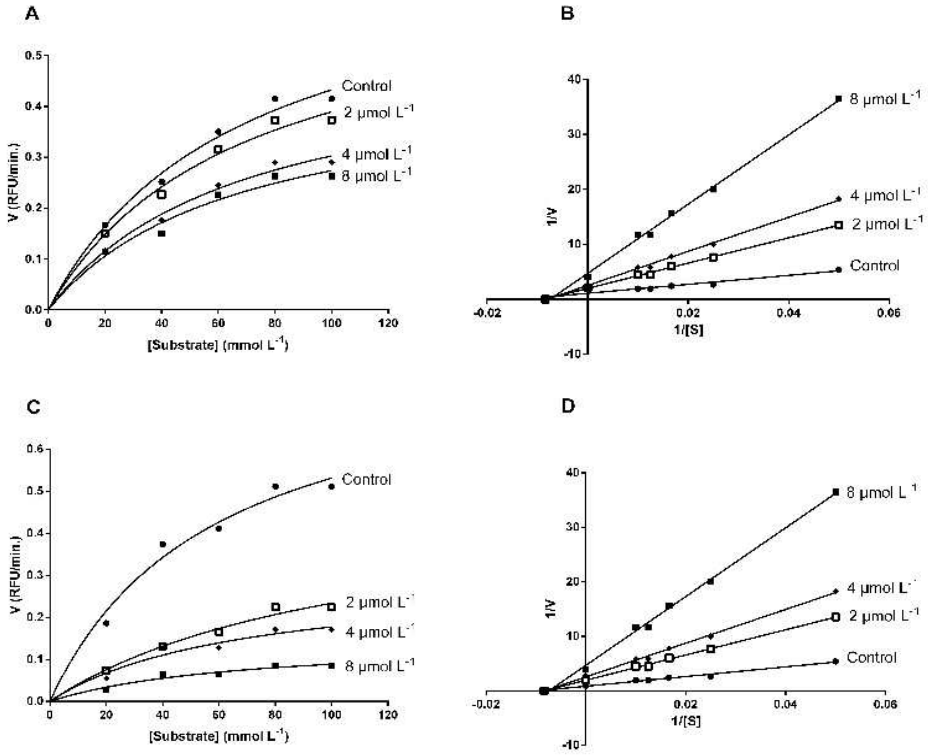

Figure 4. Enzymatic kinetics of WNV NS2-NB3 protease in the presence of compounds **14** and **17**. In **A** and **C** are shown the Michaelis-Menten plots for compounds **14** and **17**, respectively. In **B** and **D** are presented the Lineweaver-Burk plots for compounds **14** and **17**, respectively.

To propose likely binding modes for compounds **14** and **17**, we turned to molecular docking calculations. Other investigations have already identified noncompetitive inhibitors for the Flavivirus proteases, with inhibitor binding to allosteric sites with low K_i and IC_{50} values[42-46]. Taking into account the noncompetitive mode of inhibition, the possible binding site region was defined by analogy with an allosteric site previously characterized for the homologous Dengue virus type 2 protease[45, 47]. Docking studies were performed with the Induced Fit methodology of Glide[48, 49], therefore accounting for protein flexibility in the presence of ligands. A consistent binding mode was proposed for both compounds, in which ligand orientation and complex stability seem to be guided by several hydrogen bond interactions (Figure 5, Table 4). The *para*-hydroxyl group is predicted to interact with residues Trp89 and Ile147, while one of the carbonyl groups interacts with Gln167. The *meta*-hydroxyl group, present only in **17**, hydrogen bonds to Gly124. These results provide a possible explanation for the importance of

meta and *para* phenyl hydroxyl groups for effective inhibition of NS2-NB3 WNV protease, in agreement with the SAR data here reported.

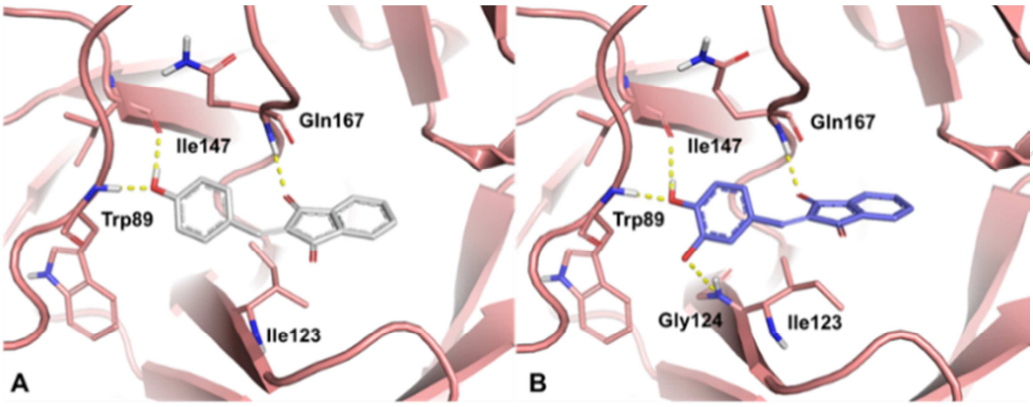

Figure 5. Docking predicted binding modes for compounds **14** (A) and **17** (B) to WNV protease. The protease is shown as cartoon, with residues involved in hydrogen bonds (Trp89, Gly124, Ile147 and Gln169) and the central residue in the grid (Ile123) highlighted as sticks and colored by atom. Hydrogen bonds are highlighted as yellow dashes.

Table 4. Predicted hydrogen bond interactions between WNV protease and compounds **14** and **17**.

Ligand atom	Compound	Interacting residue and atom	Distance(Å)[a]
p-OH	**14**	Ile147, backbone carbonyl	2.8
	17		3.2
p-OH	**14**	Trp89, backbone NH	2.8
	17		2.9
Indandione carbonyl	**14**	Gln167, backbone NH	3.2
	17		3.1
m-OH	**17**	Gly124, backbone NH	3.1

[a]distances between donor and acceptor atoms.

Considering that only two compounds (**14** and **17**) showed activity against WNV NS2-NS3 protease and based on the hypothesis that this activity could be due, in part, to the presence of the hydroxyl groups (acting as, for example, H-bond forming groups), we decided to investigate the role of such groups through some computational calculations. These two compounds are not the only ones with H-bond forming groups attached to the phenyl ring of arylidene portion.

Compounds **4**, **5**, **8**, **10**, **15** and **16**, for example, also contain small H-bond forming groups attached to the phenyl ring (nitro-, fluoro-, hidroxi-, cyano-, hidroxi- and hidroxi- groups, respectively). Besides that, compounds **6**, **12** and **13** are only methoxy-substituted, while compound **11** is a dimethylamino-compound. Therefore, all of these groups could be H-bond forming. However, the bulky substituents in **6** and **11** to **13** could hinder these compounds from interacting with the active site of WNV NS2-NS3 protease. Since compounds **8**, **15** and **16** were considerably less active than **14** and **17** (probably due to steric effects of the methyl groups) and all the remaining compounds showed no activity, we decided to treat the compounds **2** (unsubstituted; included only for comparison), **4**, **5**, **8**, **10** and **14** to **17** with computational methods.

Considering that the crystal structure of compound **15** exhibits a periplanar relation between the indan-1,3-dione and arylidene moieties, we performed a conformational analysis around the torsion between these ring systems (the C2-C10-C11-C12 dihedral angle in Figure 1). Calculations were performed based on two methods: gas phase and water implicit solvation. For both methods, we used DFT functional B3LYP and basis set 6-31G(d,p) for compounds **14**, **15** and **17**. The resulting calculations showed the same periplanar relation between the indan-1,3-dione and arylidene groups as the most stable conformations (torsions very close to zero or 180°). For computational simplicity reasons, the remaining calculations were performed exclusively in gas phase.

Compounds **2**, **4**, **5**, **8**, **10** and **14** to **17** were fully optimized in gas phase from periplanar conformations at the B3LYP/6-31G(d,p) level. Molecular electrostatic potential (MEP) surfaces were generated for all the resulting optimized geometries, as shown in Figure 6. We can see from these calculations that, for all compounds, both carbonyl groups show local negative electrostatic potentials. However, important differences are observed regarding positive electrostatic potentials. For compounds **2**, **5** and **10**, weak positive potentials are well spread over the surfaces. For the nitrocompound **4**, the positive potentials are mainly over the indan-1,3-dione system. Compounds **4**, **5** and **10** show also negative potentials over the nitro, fluoro and cyano functional groups. Finally, active compounds **8** and **14** to **17** show positive potentials over the hydrogens of hydroxyl groups. In compounds **8**, **15** and **16**, steric effects of methoxy groups could hinder better interactions with target macromolecules. Thus, compounds **14** and **17**, the most bioactives of the tested set, are the only ones to exhibit positive potentials and with no

hindrance. The values of the potentials for these two molecules, higher than the other ones, indicates that the electrostatic interactions between each of them and target macromolecules would be more efficient than the other compounds [49,50].

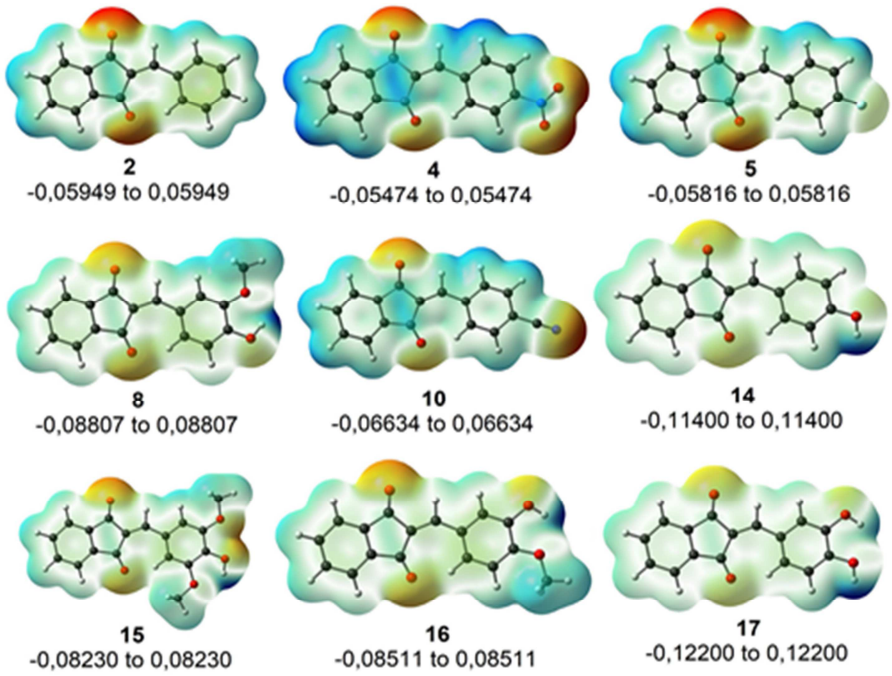

Figura 6. MEP surfaces mapped from total electron density for compounds **2**, **4**, **5**, **8**, **10** and **14** to **17**. Electrostatic potentials are displayed on a 0.002 a.u. isodensity surface. The limits of electrostatic potentials for each molecule are under surfaces. Potential increases in the following order: red (most negative) → orange → yellow → green → blue (most positive).

In the present investigation, the most bioactive compounds **14** and **17**, along with compounds **8**, **15** and **16** (which showed negligible inhibitory effect), are the only phenolic ones. This observation strengthens the hypothesis that this functional group represents an important structural feature for protease inhibition by indan-1,3-diones.

It should be mentioned that derivatives of indan-1,3-diones presenting antiviral activity for Human Papillomavirus (HPV) [50-52], Human Immunodeficiency Virus (HIV) [53] and Hepatitis C Virus (HCV) [54] have been described. Concerning HIV and HCV, the effects of the indan-1,3-dione derivatives occurred in viral replication, against HIV integrase and HCV protease. HCV is also a member of the Flaviviridae family.

The effect of compounds **14** and **17** was also assessed against Vero cell line. It was noticed that Vero cells morphology and viability were unaffected by treatment with compounds. The cytotoxicity concentration of the compounds that reduces cell viability by 50% (CC_{50}) corresponded to 89,72 μmol L^{-1} and 267,60 μmol L^{-1} for **14** and **17** respectively, demonstrating the high inhibitory potential of these derivatives. Lyu, Rhim and Park evaluated the cytotoxicity of flavonoids on Vero cells and they considered as low cytotoxic compounds those presenting CC_{50}> 50 μmol L^{-1}, which indicates that the compounds did not affect the growth of Vero cells [55].

To prove the potential antiviral efficacy of compounds **14** and **17,** we tested these active indan-1,3-diones in cellular assays against all serotypes of dengue virus, which are members of Flaviviridae family. The virucidal assay was conducted by prior incubation of the virus with the evaluated compounds. After incubation, the mixture containing the virus and thecompound under evaluation was added to the VERO cell line for a period to allow viral adsorption and internalization. Subsequently, the mixture was replaced by a semi solid medium and the development of lysis plates on VERO cells was verified. This assay was conducted using different concentrations of compounds against DENV-1-4 viruses. The concentration of test compounds that inhibited 50% of viral infection (EC_{50}) was obtained by nonlinear regression, leading to the calculation of the Selectivity Index (SI). These values are summarized in Table 3S. Compound **14**, despite having antiviral activity, did not present relevant SI values, whereas for compound **17** high SI values were observed, 34, 13, 147 and 9 DENV-1, DENV-2, DENV-3 and DENV- viruses, respectively. The results indicate that the compounds have significant antiviral efficacy and are promissing antiviral canditates.

CONCLUSIONS

It was herein described the preparation of a series of 2-arylidene indan-1,3-diones via zirconium catalyzed Knoevenagel condensation. From our point of view, the reported methodology presents the following advantages: i) it does not require the use of toxic solvents; ii) the catalyst is easy to handle, is commercially available, and presents low cost; iii) the reactions are simple to run, affords compounds in synthetically useful yields, and can be conducted in an open-air flask. Biological assays revealed that among the prepared compounds,

two of them (compounds **14** and **17**) display inhibitory activity against the NS2B-NS3 WNV protease, without any cytotoxic effect on Vero cells. The viral protease utilized in the biological assays is a very important enzyme for *Flaviviral* replication. Based on data herein described, it is clear that the compounds are non-competitive inhibitors with low IC_{50} and K_i values. To the best of our knowledge, this is the first report describing anti-WNV activity of 2-arylidene indan-1,3-dione derivatives. The potential antiviral efficacy of these compounds was demonstrated by virucidal assay against the four serotypes of dengue virus, a Flaviviridae family member like WNV.

EXPERIMENTAL SECTION

Reagents: All reagents were purchased from commercial sources (Sigma Aldrich - St. Louis, MO, US and Vetec - Rio de Janeiro, Brazil) and were employed as received. Solvents were procured from Vetec (Rio de Janeiro, Brazil) and were used as received. The 1H (300 MHz) and 13C NMR (75 MHz) spectra were recorded on a Varian Mercury 300 instrument ((Varian, Palo Alto, California, US) 300), using $CDCl_3$ and DMSO-d_6 as solvents. Hydrogen nuclear magnetic resonance (NMR) data are presented as follows: chemical shift (δ) in ppm, number of hydrogen atoms, multiplicity, *J* values in Hertz (Hz). Multiplicities are shown as the following abbreviations: s (singlet), d (doublet), dap (apparent doublet), tap (apparent triplet), ddap (apparent double of a doublet) m (multiplet). Infrared spectra (IR) were obtained employing the equipment Agilent 660-IR (Santa Clara, California) with accessory GladiATR. High resolution mass spectra were recorded on a Q-Exactive (Thermo Scientific, Bremen, Germany). The spectra were acquired using the following conditions. Ionization source: Electron spray (+) and (-); Spray voltage: 3.5 kV; Capillary temperature: 275 °C; Sheath gas: 5 (arbitrary units); Auxiliary gas: 0 (arbitrary units). For the mass spectrometry analyses, the samples were prepared as follows: a mass of 1 mg of the compound to be analyzed was dissolved in 1 mL of acetonitrile. Then, the solution was diluted with 1 mL of methanol so that the final concentration corresponded to 1 ppm. The resulting solution was directly injected in the Q-Exactive equipment at 5 µmL min-1. The spectra were recorded in full MS mode. Melting points are uncorrected and were determined using MQAPF-301 melting point apparatus (Microquimica, Rio de Janeiro, Brazil). Low resolution mass spectra were obtained on a SHIMADZU GCMS-QP5050A instrument (Kyoto, Japan) by direct injection using the following temperature program: 40 °C

min-1 until temperature reaches 60 °C, and then 80 °C min-1 until temperature reaches 300 °C; the detector temperature was 280 °C. Analytical thin layer chromatography analyses were carried out on TLC plates recovered with 60GF254 silica gel. Single-crystal X-ray diffraction data for compound 15 were acquired using a Bruker-AXS Kappa Duo diffractometer with an APEX II CCD detector. MoKα radiation from an IμS micro-source with multilayer optics was employed. After diffraction images collect and treatment, the crystallographic softwares were used as follows: SHELXS-97 [56] for structure solving, SHELXL-97 [56] for structure refinement, ORTEP-3 [57] and MERCURY [58] for structure analysis and preparation of artworks. Hydroxyl hydrogen followed a riding model for its coordinates and isotropic atomic displacement parameter, as well as all other CH hydrogens, even though it was firstly identified from the difference Fourier electron density map. Crystal structure of compound 15 was deposited with the Cambridge Crystallographic Data Centre (see Table 3 for deposit number).

Synthesis:

Synthesis of 2-(4-chlorobenzylidene)-1H-indene-1,3(2H)-dione (1): In a typical procedure, a round-bottomed flask (10 mL) was charged with indan-1,3-dione (150 mg, 1 mmol), 4-chlorobenzaldehyde (143 mg, 1 mmol), $ZrOCl_2 \cdot 8H_2O$ (12 mg, 4 mol%) and 3.00 mL of distilled water. The reaction mixture was heated to 85 °C and kept under magnetic stirring for 65 minutes. The progress of reaction was monitored by TLC analysis. After the completion of the reaction, the mixture was vacuum filtered and the residue washed with ice-cold ethanol. Compound **1** was obtained as a yellow solid in 68% yield (182 mg, 0.677 mmol) after recrystallization from dichloromethane-ethanol (1:1 v/v). Structure of **1** is supported by the following data.

Mp 176.3-177.8 ºC. IR (ATR): 3092, 3061, 1725, 1685, 1573, 1072, 733, 427 cm^{-1}. ^1H NMR (300 MHz, $CDCl_3$) δ: 7.47 (2H, d, J = 8.4 Hz), 7.81-7.83 (3H, m), 7.99-8.01 (2H, m), 8.41 (2H, d, J = 8.4 Hz). ^{13}C NMR (75 MHz, $CDCl_3$) δ: 123.39, 123.41, 129.1, 129.4, 131.5, 135.3, 135.5, 139.5, 140.1, 142.5, 145.1, 188.9, 189.9. HRMS ($M+H^+$): Calculated for $C_{16}H_{10}ClO_2$, 269.03693; found: 269.03619.

***Synthesis of derivatives 2-16*:** A similar procedure to that described for the preparation of **1** was utilized to synthesize compounds **2-16**. The structures of them are supported by the following data.

2-benzylidene-1*H*-indene-1,3(2*H*)-dione (2): Yellow solid, Mp 150.6-150.8 ºC. IR (ATR): 3066, 3026, 1726, 1681, 1609, 1584, 1564, 732, 683 cm^{-1}. ^1H NMR (300 MHz, $CDCl_3$) δ: 7.48-

7.58 (3H, m), 7.78-7.84 (2H, m), 7.89 (1H, s), 7.98-8.04 (2H, m), 8.44-8.46 (2H, m). ^{13}C NMR (75 MHz, $CDCl_3$) δ: 123.3, 123.4, 128.8, 129.2, 133.1, 133.2, 134.1, 135.1, 135.3, 140.0, 142.5, 146.9, 188.9, 190.2. HRMS ($M+H^+$): Calculated for $C_{16}H_{11}O_2$, 235.07590; found: 235.07530.

2-(4-bromobenzylidene)-1*H*-indene-1,3(2*H*)-dione (3): Yellow solid, Mp 169.7-170.3 ºC. IR (ATR): 3088, 3055, 1725, 1685, 1574, 1069, 504 cm^{-1}. ^{1}H NMR (300 MHz, $CDCl_3$) δ: 7.63 (2H,d, J = 8.7 Hz), 7.79 (1H, s), 7.81-7.83 (2H, m), 7.99-8.02 (2H, m), 8.32 (2H, d, J = 8.7 Hz). ^{13}C NMR (75 MHz, $CDCl_3$) δ: 123.41, 123.43, 128.3, 129.6, 131.9, 132.1, 135.4, 135.5, 140.1, 142.5, 145.2, 188.9, 189.9. HRMS ($M+H^+$): Calculated for $C_{16}H_{10}BrO_2$, 312.98642; found: 312.98538.

2-(4-nitrobenzylidene)-1*H*-indene-1,3(2*H*)-dione (4): Yellow solid, Mp 233.1-233.6 ºC. IR (ATR): 3109, 3076, 1732, 1688, 1566, 1514, 1345, 857 cm^{-1}. ^{1}H NMR (300 MHz, DMSO-d_6) δ: 7.93 (1H, s), 7.96-8.04 (4H, m), 8.33 (2H, d, J = 9.0 Hz), 8.58 (2H, d, J = 9.0 Hz). ^{13}C NMR (75 MHz, DMSO-d_6) δ: 123.79, 123.86, 132.9, 134.6, 136.7, 136.8, 138.9, 140.2, 142.0, 142.6, 149.3, 188.6, 189.2. MS m/z (%): 279 ([M^+], 43), 262 (76), 249 (7) 232 (100), 221 (6), 205 (17), 193 (6), 176 (63), 165 (19), 151 (24), 126 (5), 104 (41), 88 (22), 76 (56), 63 (12), 50 (55).

2-(4-fluorobenzylidene)-1*H*-indene-1,3(2*H*)-dione (5): Yellow solid, Mp 181.7 ºC. IR (ATR): 3073, 3039, 1729, 1689, 1578, 1199, 834 cm^{-1}. ^{1}H NMR (300 MHz, $CDCl_3$) δ: 7.18 (2H, t_{ap}, J = 8.7 Hz), 7.79 (1H, s), 7.80-7.83 (2H, m), 7.96-8.03 (2H, m), 8.52 (2H, dd_{ap}, J_1 = 8.7 Hz, J_2 = 5.6 Hz). ^{13}C NMR (75 MHz, $CDCl_3$) δ: 116.1 (d, $^2J_{C\text{-}F}$ = 21.8 Hz), 123.32, 123.34, 128.6, 129.6 (d, $^4J_{C\text{-}F}$ = 3.0 Hz), 135.3, 135.4, 136.9 (d,$^3J_{C\text{-}F}$ = 9.0 Hz), 140.0, 142.4, 145.4, 165.6 (d, $^1J_{C\text{-}F}$ = 255.8 Hz), 189.1, 190.1. HRMS ($M+H^+$): Calculated for $C_{16}H_{10}FO_2$, 253.06648; found: 253.06578.

2-(4-methoxybenzylidene)-1*H*-indene-1,3(2*H*)-dione (6): Yellow solid, Mp 155.3-156.8 ºC. IR (ATR): 3093, 3043, 2981, 1718, 1681, 1247, 1268, 1177, 1020, 1511, 833, 730 cm^{-1}. ^{1}H NMR (300 MHz, $CDCl_3$) δ: 3.90 (3H, s),7.00 (2H, d, J = 9.0 Hz), 7.76-7.80 (2H, m), 7.83 (1H, s), 7.93-8.00 (2H, m), 8.53 (2H, d, J = 9.0 Hz). ^{13}C NMR (75 MHz, $CDCl_3$) δ: 55.6, 114.4, 123.0, 126.4, 126.5, 134.8, 135.0, 137.1, 139.9, 142.3, 146.8, 164.0, 189.4, 190.7. HRMS ($M+H^+$): Calculated for $C_{17}H_{13}O_3$, 265.08647; found: 265.08572.

2-(benzo[*d*][1,3]dioxol-5-ylmethylene)-1*H*-indene-1,3(2*H*)-dione (7): Yellow solid, Mp 207.1-207.8 ºC. IR (ATR): 3099, 3075, 2908, 1715, 1673, 1562, 1276, 929, 724 cm^{-1}. ^{1}H NMR (300 MHz, $CDCl_3$) δ: 6.09 (2H, s),6.93 (1H, d, J = 8.4 Hz), 7.77-7.82 (4H, m), 7.94-8.00 (2H,

m), 8.51 (1H, d, *J* = 1.5 Hz). ^{13}C NMR (75 MHz, $CDCl_3$) *δ*: 102.1, 108.6, 112.8, 123.13, 123.10, 126.8, 128.1, 132.9, 134.9, 135.1, 139.9, 142.4, 146.9, 148.1, 152.4, 189.3, 190.6. HRMS ($M+H^+$): Calculated for $C_{17}H_{11}O_4$, 279.06573; found: 279.1590.

2-(4-hydroxy-3-methoxybenzylidene)-1*H*-indene-1,3(2*H*)-dione (8): Yellow solid, Mp 215.6-216.4 ºC. IR (ATR): 3535-3316 (broad band), 3085, 2974, 1719, 1679, 1572, 1278, 1255, 1154, 1017, 731 cm^{-1}. ^{1}H NMR (300 MHz, DMSO-d_6) *δ*: 3.90 (3H, s), 6.93 (1H, d, *J* = 8.4 Hz), 7.72 (1H, s), 7.86-7.94 (5H, m), 8.68 (1H, d, *J* = 1.8 Hz). ^{13}C NMR (75 MHz, DMSO-d_6) *δ*: 56.1, 116.1, 117.2, 123.1, 123.2, 125.4, 125.5, 132.1, 135.8, 135.9, 139.6,142.1, 147.3, 147.8, 153.7, 189.6, 190.4. HRMS ($M+H^+$): Calculated for $C_{17}H_{13}O_4$, 281.08138; found: 281.08072.

2-(furan-2-ylmethylene)-1*H*-indene-1,3(2*H*)-dione (9): Yellow solid, Mp 202.1-203.4 ºC. IR (ATR): 3138, 3099, 1725, 1681, 1585, 1462, 1346, 1158, 733 cm^{-1}. ^{1}H NMR (300 MHz, $CDCl_3$) *δ*: 6.68-6.80 (1H, m), 7.75-7.81 (4H, m), 7.95-7.98 (2H, m), 8.54-8.61 (1H, m). ^{13}C NMR (75 MHz, $CDCl_3$) *δ*: 114.6, 122.9, 123.1, 124.8, 129.3, 134.9, 135.1, 140.4, 142.3, 149.0, 151.4, 188.9, 190.1. HRMS ($M+H^+$): Calculated for $C_{14}H_9O_3$, 225.05517; found: 225.05455.

4-((1,3-dioxo-1*H*-inden-2(3*H*)-ylidene)methyl)benzonitrile (10): Yellow solid, Mp 233.6-235.2 ºC. IR (ATR): 3099, 3053, 2226, 1726, 1684, 1586, 842, 730 cm^{-1}. ^{1}H NMR (300 MHz, DMSO-d_6) *δ*: 7.88 (1H, s), 7.95-8.06 (6H, m), 8.53 (2H, d, *J* = 8.4 Hz). ^{13}CNMR (75 MHz, DMSO-d_6) *δ*: 114.4, 118.8, 123.7, 123.8, 132.4, 132.7, 133.9, 136.6, 136.7, 137.2, 140.1, 142.5, 142.7, 188.6, 189.2. HRMS ($M+H^+$): Calculated for $C_{17}H_{10}NO_2$, 260.07115; found: 260.07053.

2-(4-(dimethylamino) benzylidene)-1*H*-indene-1,3(2*H*)-dione (11): Red solid, Mp 180.1-181.5 ºC. IR (ATR): 3080, 3032, 2927, 1709, 1665, 1613, 1555, 1518, 1330, 1186, 815, 722 cm^{-1}. ^{1}H NMR (300 MHz, $CDCl_3$) *δ*: 3.11 (6H, s), 6.71 (2H, d, *J* = 9.1 Hz), 7.67-7.71 (2H, m), 7.75 (1H, s), 7.87-7.94 (2H, m), 8.50 (2H, d, *J* = 9.1 Hz). ^{13}C NMR (75 MHz, $CDCl_3$) *δ*: 40.0, 111.3, 121.9, 122.4, 122.9, 134.0, 134.3, 137.9, 139.8, 142.2, 147.5, 153.9, 189.9, 191.7. HRMS ($M+H^+$): Calculated for $C_{18}H_{16}NO_2$, 278.11810; found: 278.11746.

2-(3,4,5-trimethoxybenzylidene)-1*H*-indene-1,3(2*H*)-dione (12): Orange solid, Mp 185.4-185.6 ºC. IR (ATR): 3099, 3002, 2972, 2936, 1715, 1678, 1561, 1499, 1307, 1240, 1223, 1128, 732 cm^{-1}. ^{1}H NMR (300 MHz, $CDCl_3$) *δ*: 3.98 (3H, s),3.99 (6H, s), 7.78-7.81 (3H, m), 7.95 (2H, s), 7.97-7.99 (2H, m). ^{13}C NMR (75 MHz, $CDCl_3$) *δ*: 56.3, 61.0, 112.0, 123.1, 123.2, 127.7, 128.4, 135.0, 135.2, 139.8, 142.4, 143.0, 147.3, 152.8, 189.4, 190.4. HRMS ($M+H^+$): Calculated for $C_{19}H_{17}O_5$, 325.10760; found: 325.10675.

2-(3,4-dimethoxybenzylidene)-1*H*-indene-1,3(2*H*)-dione (13): Yellow solid, Mp 205.0-205.4 ºC. IR (ATR): 3088, 3010, 2972, 1712, 1671, 1565, 1505, 1271, 1247, 1141, 1019, 736 cm^{-1}. ^{1}H NMR (300 MHz, $CDCl_3$) δ: 3.97 (3H, s),4.07 (3H, s), 6.95 (1H, d, J = 8.4 Hz), 7.71-7.83 (4H, m), 7.95-7.99 (2H, m), 8.83 (1H, d_{ap}, J = 1,5 Hz). ^{13}C NMR (75 MHz, $CDCl_3$) δ: 56.1, 110.6, 115.5, 122.9, 123.0, 126.4, 126.9, 131.3, 134.8, 135.0, 139.8, 142.3, 147.4, 148.8, 153.9, 189.7, 190.7. HRMS ($M+H^+$): Calculated for $C_{18}H_{15}O_4$, 295.09703; found: 295.09650.

2-(4-hydroxybenzylidene)-1*H*-indene-1,3(2*H*)-dione (14): Yellow solid, Mp 235.8-236.0 ºC. IR (ATR): 3059, 1715, 1655, 1547, 1505, 1204, 737 cm^{-1}. ^{1}H NMR (300 MHz, DMSO-d_6) δ: 6.92 (2H, d, J = 8.7 Hz), 7.72 (1H, s), 7.86-7.92 (4H, m), 8.50 (2H, d, J = 8.7 Hz), 10.86 (1H, s). ^{13}C NMR (75 MHz, DMSO-d_6) δ: 116.4, 123.1, 123.2, 125.0, 125.6, 135.8, 135.9, 138.0, 139.6, 142.0, 146.7, 163.7, 189.4, 190.4. HRMS ($M-H^-$): Calculated for $C_{16}H_9O_3$, 249.05517; found: 249.05568.

2-(4-hydroxy-3,5-dimethoxybezylidene)-1*H*-indene-1,3(2*H*)-dione (15): Orange solid, Mp 222.4-223.1 ºC. IR (ATR): 3545-3197 (broad band), 3093, 3010, 2941, 1712, 1667, 1565, 1503, 1318, 1227, 1083, 732 cm^{-1}. ^{1}H NMR (300 MHz, DMSO-d_6) δ: 3.88 (6H, s), 7.74 (1H, s), 7.85-7.93 (4H, m), 8.13 (2H, s). ^{13} CNMR (75 MHz, DMSO-d_6) δ: 56.5, 113.2, 123.1, 123.2, 124.2, 125.7, 135.8, 135.9, 139.6, 142.2, 143.1, 147.8, 147.9, 189.7, 190.4. HRMS ($M+H^+$): Calculated for $C_{18}H_{15}O_5$, 311.09195; found: 311.09131.

2-(3-hydroxy-4-methoxybenzylidene)-1*H*-indene-1,3(2*H*)-dione (16): Yellow solid, Mp 219.0-219.2 ºC. IR (ATR): 3546-3288, 3072, 2989, 1718, 1681, 1574, 1498, 1276, 1219, 1137, 734 cm^{-1}. ^{1}H NMR (300 MHz, DMSO-d_6) δ: 3.89 (3H, s), 7.09 (1H, d, J = 8.6 Hz), 7.67 (1H, s), 7.87-7.95 (5H, m), 8.28 (1H, d_{ap}, J = 1.9 Hz). ^{13}C NMR (75 MHz, DMSO-d_6) δ: 56.3, 112.2, 120.3, 123.2, 126.4, 126.6, 130.0, 135.9, 136.1, 139.7, 142.2, 146.7, 146.9, 153.7, 189.3, 190.3. HRMS ($M+H^+$): Calculated for $C_{17}H_{13}O_4$, 281.08138; found: 281.08052.

Synthesis of 2-(3,4-dihydroxybenzylidene)-1H-indene-1,3(2H)-dione (17): To a bitubulated round bottomed flask (150 mL), under a nitrogen atmosphere, it was added compound **13** (200 mg, 0.679 mmol) along with 5.0 mL of anhydrous dichloromethane. The resulting mixture was kept under magnetic stirring and cooled in an ice bath for 40 minutes. Then, 2.7 mL of 1.00 mol L^{-1} solution of BBr_3 in dichloromethane was added dropwise. After the addition, the reaction mixture was kept under stirring for 24 hours at room temperature. Subsequently, 10.0 mL of distilled water were added and a brown precipitate formed. The resulting mixture was transferred

to a separatory funnel and the aqueous phase was extracted with ethyl acetate (3 x 30.0 mL). The organic extracts were combined, and the resulting organic phase was dried over anhydrous sodium sulfate, filtered and concentrated under reduced pressure. Compound **17** was obtained as a yellow solid after washing with dichloromethane and acetone in 58% yield (105 mg, 0.394 mmol).

Mp 238.0-239.4 ºC. IR (ATR): 3492-3109, 3093, 3039, 1720, 1666, 1555, 1384, 1182, 730 cm^{-1}. ^{1}H NMR (300 MHz, $CDCl_3$) δ: 6.89 (1H, d, J = 8.1 Hz),7.64 (1H, s), 7.83 (1H, dd, J_1 = 8.1 Hz, J_2 = 1.8 Hz), 7.86-7.94 (4H, m), 8.32 (1H, d_{ap}, J = 1.8 Hz), . ^{13}C NMR (75 MHz, $CDCl_3$) δ: 116.2, 121.0, 123.1, 125.2, 125.5, 130.7, 135.7, 135.9, 139.6, 142.1, 145.7, 147.3, 153.0, 189.4, 190.5. HRMS ($M-H^-$): Calculated for $C_{16}H_9O_4$, 265.05008; found: 265.05060.

Biological assays

Evaluation of the activity of compounds 1–17 against WNV NS2B-NS3 protease: Recombinant WNV NS2B-NS3 protease (catalog number SE-2907, already purified and activated) and fluorescent substrate pERTKR-AMC (catalog number ES013) were purchased from (R & D Systems, Minneapolis, MN, USA,). Compounds **1**–**17** were dissolved in pure DMSO; solutions were then diluted in buffer to obtain working solutions with a final concentration of DMSO of 1% v/v. A volume of 50 μL of the purified protease (final concentration of 1 ng μL^{-1}) diluted in buffer (50 mmol L^{-1} Tris, 30% (v/v) glycerol, pH 9.5) was incubated with 50 μL of DMSO solution of each indan-1,3-dione derivative (final concentration of 16 μmol L^{-1}) in a 96-well black plate for 30 min at 21–22 °C. After this time, the assay was initiated by addition of 50 μL of the substrate (40 mmol L^{-1} - initial concentration). A solution containing buffer and DMSO was used as negative control on the same plate. The blank contained 50 μL buffer and 100 μL of the substrate. The fluorescence intensity was continuously recorded on a wavelength of excitation of 360 nm and an emission wavelength of 460 nm using SpectraMax® M5 reader (Molecular Devices). Compounds, which effectively inhibit the enzyme were selected for further biological assays. Analyses were performed using Microsoft Excel (Microsoft Office Software) and GraphPad Prism 6 (GraphPad Software Inc.). The assays were conducted in triplicated on three isolated experiments and the statistical analyses were conducted by utilizing the multiple comparisons of one-way ANOVA.

Determination of IC_{50} values: The inhibitory enzymatic activity of compounds **14** and **17**, the most active ones against the WNV NS2-NB3 protease, were evaluated at eight different

concentrations (66 μmol L^{-1}–0.5 μmol L^{-1}) using the protease assay as described above. Fluorescence was measured in triplicate wells at intervals of 30 s for 5 min in three independent experiments. IC_{50} values were calculated using GraphPad Prism 6 GraphPad Software Inc.), using the four-parameter nonlinear regression analysis (Hill slope method).

Determination of K_i values: Three different concentrations (2, 4 and 8 μmol L^{-1}) of inhibitors **14** and **17** and five different concentrations of substrate pERTKR-AMC (20, 40, 60, 80, 100 mmol L^{-1}) were tested in the *in vitro* against WNV protease (37.04 nmol L^{-1} protein, 1 ng μL^{-1}). Fluorescence was measured in triplicate wells at an interval of 30 s. The velocity values (RFU/minute) were then calculated for each substrate/inhibitor pair. K_i values were calculated with GraphPad Prism software 6 (GraphPad Software Inc.) with non-linear regression at competitive inhibition mode of enzyme-kinetics.

Cytotoxicity assay: The cytotoxicity of compounds **14** and **17** was assessed using MTT assay[59]. VERO cells (5 x 10^4 cells) were seeded in 96-well plates. Each well contained 100 µL of each compound solution at different concentrations (1000, 250, 125, 63, 32, 17, 8 and 4 μmol L^{-1}). The compounds were diluted in MEM medium with 2% FBS and 1% DMSO. After 24 h of incubation at 37 ^{o}C, 100 μL of a MTT solution (5%) was added to the wells. After 4 h at 37 ºC, the MTT solution was removed and 100 µL/well of DMSO was added to solubilize the formazan. Absorbance was measure at 550 nm was measured in a microplate reader (Multiskan™ GO Microplate Spectrophotometer – ThermoFisher®). The data were analyzed and CC_{50} was determined using GraphPad Prism 6 (GraphPad Software Inc.).

Virucidal assay: VERO cells (8 x 10^5 cells per well) were seeded in 24-well plates. 100 µL of viral suspension (50-100 PFU) were incubated with 100 µL of varying concentrations of the tested compounds (3, 6, 12, 25, 50 and 100 µmol L^{-1}) and incubated at 37 ° C for 1 h. The medium was aspirated from the plates and 100 µL of the mixture contaning the virus and the compound mixture was added to the cell monolayer. The plates were incubated for 1 hour under shaking for a better viral distribution. After this time, the viral suspension mixed at the various concentrations of the evaluated compound was aspirated and 1500 µL of a 3% CMC solution in DMEM (twice concentrated) medium supplemented with 2% FBS and 1% PSA was added to each well. Plates were incubated for 5-6 days. After this period, the medium was removed and the cells fixed by adding formaldehyde 20% for 30 minutes at 37 ºC and stained by adding 2 to 3 drops of 5% violet crystal dye for 40 minutes at room temperature on a mechanical stirrer. After

this time, the dye was aspirated and the plates were placed to dry at room temperature and quantified by visualization of lysis plates. The data were analyzed and EC_{50} was determined using GraphPad Prism 6 (GraphPad Software Inc.). With the value of CC_{50} and EC_{50} in hands, it was possible to calculate the value of the selectivity index (SI), which corresponds to the ratio CC_{50}/EC_{50}.

Computational analyses

Conformational analyzes, optimizations and electrostatic potential calculations: Molecules were prepared in the program GaussView 5.0.8 [60]. Conformational analyses and geometries optimizations were performed with the software Gaussian 09W [61]. Implicit solvation calculations were run using the IEF-PCM model. Total electron density and molecular electrostatic potential surfaces were generated from Gaussian outputs with GaussView.

Docking studies: Ligands were prepared in the program Ligprep [62] employing the OPLS_2005 force field, with protonation states predicted with Epik at pH 9.5 ± 2.0. The West Nile virus protease NS2B-NS3 PDB code 2FP7[63], chosen as the receptor, was prepared with the Protein Preparation Wizard (Schrödinger Release 2015-3: Schrödinger Suite 2015-3 Protein Preparation Wizard; Epik version 3.3, Schrödinger, version 6.8) [64], with removal of all waters and addition of hydrogens based on PROPKA calculations at pH 9.5. Docking calculations were performed with the software Glide (Small-Molecule Drug Discovery Suite 2015-4: Glide, version 6.8) [48], employing the Induced Fit docking methodology [49] and Glide SP. The grid was centered in the amino acid Isoleucine 123, and had 12 Å dimensions. All residues within 5 Å from Ile123 were considered as flexible. Docking results were ranked based on their docking score and the top ranking poses for each compound were analyzed with the software PyMOL [65].

AUTHOR CONTRIBUTIONS

The manuscript was written through contributions of all authors. All authors have given approval to the final version of the manuscript. AFCSO and ASO were responsible for all in vitro assays with WNV protease with the assistance of EGS and IEPS under the supervision of SOP. APMS performed the synthesis of the compounds with the assistence of MLS under the supervision of

RRT. RSF and FTM performed the docking studies. DHSL conducted the molecular electrostatic potential analysis. BGV was responsible for the acquisition of high resolution mass spectra. FTM performed the acquisition and interpretation of crystallographic data.

FUNDING SOURCES

This work was supported by National Counsel of Technological and Scientific Development (CNPq), Foundation for Supporting Research in the state of Minas Gerais (FAPEMIG) and by the National Program for Academic Cooperation (PROCAD) of the Coordination for the Improvement of Higher Education Personnel-CAPES/Brazil.

ACKNOWLEDGMENT

D. H. S. Leal would like to thank the Computational Chemistry Group from Universidade Federal de Lavras for the use of softwares (Gaussian and GaussView) and computers in this work.

REFERENCES

[1] E. knoevenagel, Ueber eine Darstellungsweise der Glutarsaure, Chem. Ber., (1894) 2345-2346.
[2] E. knoevenagel, Condensation von Malondiure mit Aromatiachen Aldehyden durch Ammoniak und Amine, Beri deuts chem Gesel, (1898) 2596-2619.
[3] L. Kürti, B. Czakó, Strategic Application of Named Reactions in Organic Synthesis, Elsevier Academic Press, Amsterdam, 2005.
[4] N. Yu, J.M. Aramini, M.W. MGermann, Z. Huang, Reactions of salicylaldehydes with alkyl cyanoacetates on the surface of solid catalysts:syntheses of 4H-chromene derivatives, Tetrahedron Lett., (2000) 6993-6996.
[5] F. Bigi, L. Chesini, R. Maggi, G. Sartori, Montmorillonite KSF as an Inorganic, Water Stable, and Reusable Catalyst for the Knoevenagel Synthesis of Coumarin-3-carboxylic Acids, J. Org. Chem., 64 (1999) 1033-1035.
[6] A.E. Morrison, T.T. Hoang, M. Birepinte, G.B. Dudley, Synthesis of Illudinine from Dimedone, Org. Lett., 19 (2017) 858-861.
[7] Y. Ogiwara, K. Takahashi, T. Kitazawa, N. Sakai, Indium(III)-catalyzed knoevenagel condensation of aldehydes and activated methylenes using acetic anhydride as a promoter, J. Org. Chem., 80 (2015) 3101-3110.
[8] F. Shirini, M.A. Zolfigol, E. Mollarazi, 53KBrO3/ZrClO2 • 8H2O: An efficient reagent system for the oxidation of alcohols, Synth. Commun., 35 (2005) 1541-1545.
[9] M. Nakayama, A. Sato, K. Ishihara, H. Yamamoto, Water-Tolerant and Reusable Catalysts for Direct Ester Condensation between Equimolar Amounts of Carboxylic Acids and Alcohols, Adv. Synth. Catal., 346 (2004) 1275-1279.

[10] I. Mohammadpoor-Baltork, A.R. Khosropour, S.F. Hojati, ZrOCl2.8H2O as an environmentally friendly and recyclable catalyst for the chemoselective synthesis of 2-aryloxazolines and bis-oxazolines under thermal conditions and microwave irradiation, Catal. Commun., 8 (2007) 200-204.
[11] Z.-H. Zhang, T.-S. Li, J.-J. Li, Synthesis of enaminones and enamino esters catalysed by ZrOCl2.8H2O Catal. Commun., 8 (2007) 1615-1620.
[12] M. Shi, S.-C. Cui, W.-P. Yin, Highly Efficient Catalytic Nitration of Phenolic Compounds by Nitric Acid with a Recoverable and Reusable Zr or Hf Oxychloride Complex and KSF, Eur. J. Org. Chem., (2005) 2349-2384.
[13] R. Ghosh, S. Maiti, A. Chakraborty, Facile catalyzed acylation of alcohols, phenols, amines and thiols based on ZrOCl2·8H2O and acetyl chloride in solution and in solvent-free conditions, Tetrahedron Lett., 46 (2005) 147-151.
[14] R. Ghosh, S. Maiti, A. Chakraborty, S. Chakraborty, A.K. Mukherjee, Tetrahedron, 62 (2006) 4059-4064.
[15] H.B. Sun, R. Hua, Y. Yin, ZrOCl2 x 8H2O: an efficient, cheap and reusable catalyst for the esterification of acrylic acid and other carboxylic acids with equimolar amounts of alcohols, Molecules, 11 (2006) 263-271.
[16] H. Firouzabadi, N. Iranpoor, M. Jafarpour, A. Ghaderi, ZrOCl2.8H2O as a highly efficient and the moisture tolerant Lewis acid catalyst for Michael addition of amines and indoles to α, β-unsaturated ketones under solvent-free conditions, J. Mol.Catal. , 252 (2006) 150-155.
[17] M.M. Hashemi, B. Eftekhari-Sis, A. Abdollahifar, B. Khalili, ZrOCl2· 8H2O on montmorillonite K10 accelerated conjugate addition of amines to α, β-unsaturated alkenes under solvent-free conditions, Tetrahedron, 62 (2006) 672-677.
[18] b. Eftekhari-Sis, a. Abdollahifar, M.M. Hashemi, M. Zirak, Stereoselective Synthesis of β-Amino Ketones via Direct Mannich-Type Reactions, Catalyzed with ZrOCl2 · 8 H2O under Solvent-Free Conditions, Eur. J. Org. Chem., (2006) 5152-5157.
[19] J.C. Rodríguez-Domínguez, D. Bernardi, G. Kirsch, ZrCl4 or ZrOCl2 under neat conditions: optimized green alternatives for the Biginelli reaction, Tetrahedron Lett., 48 (2007) 5777-5780.
[20] I. Mohammadpoor-Baltork, A.R. Khosropour, S.F. Hojati, ZrOCl2·8H2O as an efficient, environmentally friendly and reusable catalyst for synthesis of benzoxazoles, benzothiazoles, benzimidazoles and oxazolo[4,5-b]pyridines under solvent-free conditions, Catal. Commun., 8 (2007) 1865-1870.
[21] Y. Wu, L.-N. He, Y. Du, J.-Q. Wang, C.-X. Miao, W. Li, Zirconyl chloride: an efficient recyclable catalyst for synthesis of 5-aryl-2-oxazolidinones from aziridines and CO2 under solvent-free conditions, Tetrahedron, 65 (2009) 6204-6210.
[22] B. Karami, M. Kiani, ZrOCl2.8H2O/SiO2: An efficient and recyclable catalyst for the preparation of coumarin derivatives by Pechmann condensation reaction, Catal. Commun., 14 (2011) 62-67.
[23] M.A. Martin-Acebes, A. Vazquez-Calvo, J.C. Saiz, Lipids and flaviviruses, present and future perspectives for the control of dengue, Zika, and West Nile viruses, Prog. Lipid Res., 64 (2016) 123-137.
[24] A. Chaskopoulou, C.I. Dovas, S.C. Chaintoutis, J. Kashefi, P. Koehler, M. Papanastassopoulou, Detection and early warning of West Nile Virus circulation in Central Macedonia, Greece, using sentinel chickens and mosquitoes, Vector Borne Zoonotic Dis., 13 (2013) 723-732.

[25] A. Chaskopoulou, G. L'Ambert, D. Petric, R. Bellini, M. Zgomba, T.A. Groen, L. Marrama, D.J. Bicout, Ecology of West Nile virus across four European countries: review of weather profiles, vector population dynamics and vector control response, Parasit Vectors, 9 (2016) 482.
[26] M.A. Morales, M. Barrandeguy, C. Fabbri, J.B. Garcia, A. Vissani, K. Trono, G. Gutierrez, S. Pigretti, H. Menchaca, N. Garrido, N. Taylor, F. Fernandez, S. Levis, D. Enria, West Nile virus isolation from equines in Argentina, 2006, Emerg. Infect. Dis., 12 (2006) 1559-1561.
[27] B.K. Kleinschmidt-DeMasters, J.D. Beckham, West Nile Virus Encephalitis 16 Years Later, Brain Pathol., 25 (2015) 625-633.
[28] T. Ometto, E.L. Durigon, J. de Araujo, R. Aprelon, D.M. de Aguiar, G.T. Cavalcante, R.M. Melo, J.E. Levi, S.M. de Azevedo Junior, M.V. Petry, I.S. Neto, P. Serafini, E. Villalobos, E.M. Cunha, C. Lara Mdo, A.F. Nava, M.S. Nardi, R. Hurtado, R. Rodrigues, A.L. Sherer, F. Sherer Jde, M.P. Geraldi, M.M. de Seixas, C. Peterka, S. Bandeira Dde, J. Pradel, N. Vachiery, M.B. Labruna, L.M. de Camargo, R. Lanciotti, T. Lefrancois, West Nile virus surveillance, Brazil, 2008-2010, Trans. R. Soc. Trop. Med. Hyg., 107 (2013) 723-730.
[29] S.M. Costa, A.S. Azevedo, M.V. Paes, F.S. Sarges, M.S. Freire, A.M. Alves, DNA vaccines against dengue virus based on the ns1 gene: the influence of different signal sequences on the protein expression and its correlation to the immune response elicited in mice, Virology, 358 (2007) 413-423.
[30] K.F. Teo, P.J. Wright, Internal proteolysis of the NS3 protein specified by dengue virus 2, J. Gen. Virol., 78 (Pt 2) (1997) 337-341.
[31] A.S. Oliveira, M.L. Silva, A.F.C.S. Oliveira, C.C. Silva, R.R. Teixeira, S.O.D. Paula, NS3 and NS5 proteins: important targets for anti-dengue drug design, J. Braz. Chem. Soc, 25 (2014) 1759-1769.
[32] S.P. Lim, Q.Y. Wang, C.G. Noble, Y.L. Chen, H. Dong, B. Zou, F. Yokokawa, S. Nilar, P. Smith, D. Beer, J. Lescar, P.Y. Shi, Ten years of dengue drug discovery: progress and prospects, Antiviral Res., 100 (2013) 500-519.
[33] D. Luo, S.G. Vasudevan, J. Lescar, The flavivirus NS2B-NS3 protease-helicase as a target for antiviral drug development, Antiviral Res., 118 (2015) 148-158.
[34] A. Bastos Lima, M.A. Behnam, Y. El Sherif, C. Nitsche, S.M. Vechi, C.D. Klein, Dual inhibitors of the dengue and West Nile virus NS2B-NS3 proteases: Synthesis, biological evaluation and docking studies of novel peptide-hybrids, Bioorg. Med. Chem., 23 (2015) 5748-5755.
[35] M.Z. Hammamy, C. Haase, M. Hammami, R. Hilgenfeld, T. Steinmetzer, Development and characterization of new peptidomimetic inhibitors of the West Nile virus NS2B-NS3 protease, ChemMedChem, 8 (2013) 231-241.
[36] M.A. Behnam, C. Nitsche, V. Boldescu, C.D. Klein, The Medicinal Chemistry of Dengue Virus, J. Med. Chem., 59 (2016) 5622-5649.
[37] A.K. Timiri, B.N. Sinha, V. Jayaprakash, Progress and prospects on DENV protease inhibitors, Eur. J. Med. Chem., 117 (2016) 125-143.
[38] L.F. Weigel, C. Nitsche, D. Graf, R. Bartenschlager, C.D. Klein, Phenylalanine and Phenylglycine Analogues as Arginine Mimetics in Dengue Protease Inhibitors, J. Med. Chem., 58 (2015) 7719-7733.
[39] B. Elmuradov, K.A. Bozorov, R.Y. Okmanov, B. Tashkhodjaev, K.M. Shakhidoyatov, 2-Methyl-4-oxo-6,7,8,9-tetrahydro-thieno[2',3':4,5]pyrimidino-[1,2-a]pyridine-3-c arboxylic acid, Acta Crystallogr Sect E Struct Rep Online, 67 (2011) o824.

[40] H. Petrokova, J. Duskova, J. Dohnalek, T. Skalova, E. Vondrackova-Buchtelova, M. Soucek, J. Konvalinka, J. Brynda, M. Fabry, J. Sedlacek, J. Hasek, Role of hydroxyl group and R/S configuration of isostere in binding properties of HIV-1 protease inhibitors, Eur. J. Biochem., 271 (2004) 4451-4461.
[41] S.M. Tomlinson, S.J. Watowich, Use of parallel validation high-throughput screens to reduce false positives and identify novel dengue NS2B-NS3 protease inhibitors, Antiviral Res., 93 (2012) 245-252.
[42] H. Wu, S. Bock, M. Snitko, T. Berger, T. Weidner, S. Holloway, M. Kanitz, W.E. Diederich, H. Steuber, C. Walter, D. Hofmann, B. Weissbrich, R. Spannaus, E.G. Acosta, R. Bartenschlager, B. Engels, T. Schirmeister, J. Bodem, Novel dengue virus NS2B/NS3 protease inhibitors, Antimicrob. Agents Chemother., 59 (2015) 1100-1109.
[43] L.R. de Sousa, H. Wu, L. Nebo, J.B. Fernandes, M.F. da Silva, W. Kiefer, M. Kanitz, J. Bodem, W.E. Diederich, T. Schirmeister, P.C. Vieira, Flavonoids as noncompetitive inhibitors of Dengue virus NS2B-NS3 protease: inhibition kinetics and docking studies, Bioorg. Med. Chem., 23 (2015) 466-470.
[44] C.H. Heh, R. Othman, M.J. Buckle, Y. Sharifuddin, R. Yusof, N.A. Rahman, Rational discovery of dengue type 2 non-competitive inhibitors, Chem. Biol. Drug Des., 82 (2013) 1-11.
[45] R. Othman, T.S. Kiat, N. Khalid, R. Yusof, E.I. Newhouse, J.S. Newhouse, M. Alam, N.A. Rahman, Docking of noncompetitive inhibitors into dengue virus type 2 protease: understanding the interactions with allosteric binding sites, J. Chem. Inf. Model., 48 (2008) 1582-1591.
[46] S. Sidique, S.A. Shiryaev, B.I. Ratnikov, A. Herath, Y. Su, A.Y. Strongin, N.D. Cosford, Structure-activity relationship and improved hydrolytic stability of pyrazole derivatives that are allosteric inhibitors of West Nile Virus NS2B-NS3 proteinase, Bioorg. Med. Chem. Lett., 19 (2009) 5773-5777.
[47] M. Yildiz, S. Ghosh, J.A. Bell, W. Sherman, J.A. Hardy, Allosteric inhibition of the NS2B-NS3 protease from dengue virus, ACS Chem. Biol., 8 (2013) 2744-2752.
[48] R.A. Friesner, J.L. Banks, R.B. Murphy, T.A. Halgren, J.J. Klicic, D.T. Mainz, M.P. Repasky, E.H. Knoll, M. Shelley, J.K. Perry, D.E. Shaw, P. Francis, P.S. Shenkin, Glide: a new approach for rapid, accurate docking and scoring. 1. Method and assessment of docking accuracy, J. Med. Chem., 47 (2004) 1739-1749.
[49] W. Sherman, T. Day, M.P. Jacobson, R.A. Friesner, R. Farid, Novel procedure for modeling ligand/receptor induced fit effects, J. Med. Chem., 49 (2006) 534-553.
[50] N. Goudreau, D.R. Cameron, R. Deziel, B. Hache, A. Jakalian, E. Malenfant, J. Naud, W.W. Ogilvie, J. O'Meara, P.W. White, C. Yoakim, Optimization and determination of the absolute configuration of a series of potent inhibitors of human papillomavirus type-11 E1-E2 protein-protein interaction: a combined medicinal chemistry, NMR and computational chemistry approach, Bioorg. Med. Chem., 15 (2007) 2690-2700.
[51] W. Davidson, G.A. McGibbon, P.W. White, C. Yoakim, J.L. Hopkins, I. Guse, D.M. Hambly, L. Frego, W.W. Ogilvie, P. Lavallee, J. Archambault, Characterization of the binding site for inhibitors of the HPV11 E1-E2 protein interaction on the E2 transactivation domain by photoaffinity labeling and mass spectrometry, Anal. Chem., 76 (2004) 2095-2102.
[52] C. Yoakim, W.W. Ogilvie, N. Goudreau, J. Naud, B. Hache, J.A. O'Meara, M.G. Cordingley, J. Archambault, P.W. White, Discovery of the first series of inhibitors of human papillomavirus type 11: inhibition of the assembly of the E1-E2-Origin DNA complex, Bioorg. Med. Chem. Lett., 13 (2003) 2539-2541.

[53] M. Artico, R. Di Santo, R. Costi, E. Novellino, G. Greco, S. Massa, E. Tramontano, M.E. Marongiu, A. De Montis, P. La Colla, Geometrically and conformationally restrained cinnamoyl compounds as inhibitors of HIV-1 integrase: synthesis, biological evaluation, and molecular modeling, J. Med. Chem., 41 (1998) 3948-3960.
[54] Y. Liu, A. Saldivar, J. Bess, L. Solomon, C.M. Chen, R. Tripathi, L. Barrett, P.L. Richardson, A. Molla, W. Kohlbrenner, W. Kati, Investigating the origin of the slow-binding inhibition of HCV NS3 serine protease by a novel substrate based inhibitor, Biochemistry, 42 (2003) 8862-8869.
[55] S.Y. Lyu, J.Y. Rhim, W.B. Park, Antiherpetic activities of flavonoids against herpes simplex virus type 1 (HSV-1) and type 2 (HSV-2) in vitro, Arch. Pharm. Res., 28 (2005) 1293-1301.
[56] G.M. Sheldrick, A short history of SHELX, Acta Crystallogr. A, 64 (2008) 112-122.
[57] L.J. Farrugia, WinGX and ORTEP for Windows: an update, J. Appl. Crystallogr., 45 (2012) 849-854.
[58] C.F. Macrae, I.J. Bruno, J.A. Chisholm, P.R. Edgington, P. McCabe, E. Pidcock, L. Rodriguez-Monge, R. Taylor, J. van de Streek, P.A. Wood, Mercury CSD 2.0 - New Features for the Visualization and Investigation of Crystal Structures, J. Appl. Crystallogr., 41 (2008) 466-470.
[59] T. Mosmann, Rapid colorimetric assay for cellular growth and survival: application to proliferation and cytotoxicity assays, J. Immunol. Methods, 65 (1983) 55-63.
[60] GaussView, in: R. Dennington, T. Keith, J. Millam (Eds.), Semichem Inc, Shawnee Mission, 2009.
[61] Gaussian09, in: M.J. Frisch, G.W. Trucks, H.B. Schlegel, G.E. Scuseria, M.A. Robb, J.R. Cheeseman, G. Scalmani, V. Barone, G.A. Petersson, H. Nakatsuji, X. Li, M. Caricato, A. Marenich, J. Bloino, B.G. Janesko, R. Gomperts, B. Mennucci, H.P. Hratchian, J.V. Ortiz, A.F. Izmaylov, J.L. Sonnenberg, D. Williams-Young, F. Ding, F. Lipparini, F. Egidi, J. Goings, B. Peng, A. Petrone, T. Henderson, D. Ranasinghe, V.G. Zakrzewski, J. Gao, N. Rega, G. Zheng, W. Liang, M. Hada, M. Ehara, K. Toyota, R. Fukuda, J. Hasegawa, M. Ishida, T. Nakajima, Y. Honda, O. Kitao, H. Nakai, T. Vreven, K. Throssell, J. Montgomery, J.A., J.E. Peralta, F. Ogliaro, M. Bearpark, J.J. Heyd, E. Brothers, K.N. Kudin, V.N. Staroverov, T. Keith, R. Kobayashi, J. Normand, K. Raghavachari, A. Rendell, J.C. Burant, S.S. Iyengar, J. Tomasi, M. Cossi, J.M. Millam, M. Klene, C. Adamo, R. Cammi, J.W. Ochterski, R.L. Martin, K. Morokuma, O. Farkas, J.B. Foresman, D.J. Fox (Eds.), Gaussian, Inc., Wallingford, 2016.
[62] S.R. LigPrep, in, Schrödinger, LLC, New York, 2015.
[63] P. Erbel, N. Schiering, A. D'Arcy, M. Renatus, M. Kroemer, S.P. Lim, Z. Yin, T.H. Keller, S.G. Vasudevan, U. Hommel, Structural basis for the activation of flaviviral NS3 proteases from dengue and West Nile virus, Nat. Struct. Mol. Biol., 13 (2006) 372-373.
[64] G.M. Sastry, M. Adzhigirey, T. Day, R. Annabhimoju, W. Sherman, Protein and ligand preparation: parameters, protocols, and influence on virtual screening enrichments, J. Comput. Aided Mol. Des., 27 (2013) 221-234.
[65] T.P.M.G. System, in, Schrödinger, LLC, New York, 2015.

TABLE OF CONTENTS GRAPHIC

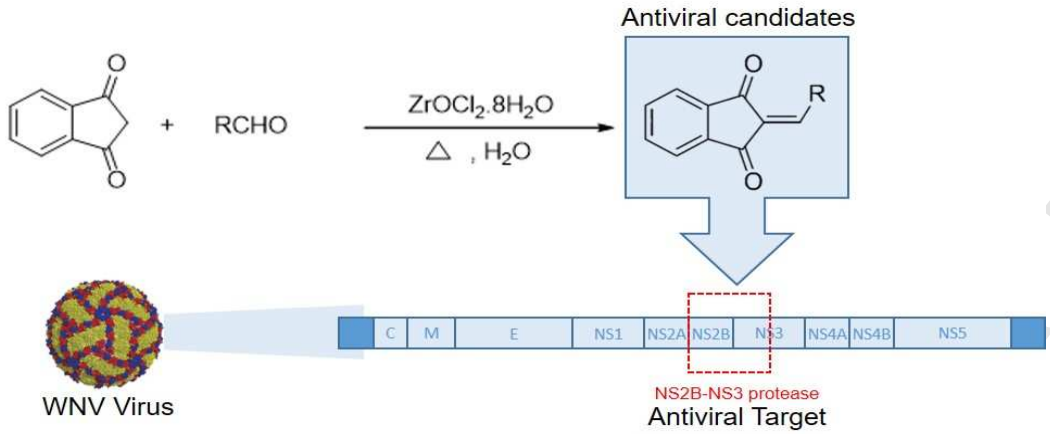

Inhibitory Activity against NS2B-NS3 WNV protease by 2-Arylidene Indan-1,3-diones synthesis by Zirconium Catalyzed

Highlights

A simple and efficient Knoevenagel procedure for the synthesis of 2-arylidene indan-1,3-diones is herein reported.

The synthesized compounds were evaluated as inhibitors of the NS2B-NS3 protease of West Nile Virus (WNV).

The most active hydroxylated derivatives, namely 2-(4-hydroxybenzylidene)-1*H*-indene-1,3(2*H*)-dione (**14**) and 2-(3,4-dihydroxybenzylidene)-1*H*-indene-1,3(2*H*)-dione (**17**), were characterized as noncompetitive enzymes inhibitors, with IC_{50} values of 11 μmol L^{-1} and 3 μmol L^{-1}, respectively.

Docking and electrostatic potential surfaces investigations provided insight on the possible binding mode of the most active compounds within an allosteric site.

To the best of our knowledge, this is the first report describing anti-WNV activity of 2-arylidene indan-1,3-dione derivatives.